

Synthesis and Antiproliferative Activity of 2-amino-4-Anilinoquinazoline Derivatives

Ravez S^{1,2}, Schifano-Faux N^{1,3}, Barczyk A^{1,2}, Arsenlis S¹⁻³, Castillo Aguilera O¹⁻³, Baldeyrou B^{1,4}, Lansiaux A^{1,4}, Six P^{1,2}, Goossens JF^{1,3}, Depreux P¹⁻³ and Goossens L^{1-3*}

¹Univ Lille, F-59000 Lille, France

²Institut de Chimie Pharmaceutique Albert Lespagnol (ICPAL), France

³UDSL, EA GRITA, F-59000 Lille, France

⁴Unité Tumorigenèse et Résistance aux Traitements, INSERM U-908, Centre Oscar Lambret, IRCL, F-59045 Lille, France

Abstract

Recently, we have reported a series of 4-anilino-6,7-dimethoxyquinazolines as tyrosine kinase inhibitors with interesting *in vitro* IC₅₀ values for the Epidermal Growth Factor Receptor (EGFR) and/or for the Vascular Endothelial Growth Factor Receptor-2 (VEGFR-2). In this paper, we studied the impact of amino group in C-2 position of the quinazoline core on this series. The new synthesized compounds described herein were evaluated for both *in vitro* EGFR and VEGFR-2 kinase inhibition and antiproliferative activity in different cancer cell lines (PC3, HT29 and MCF7). 2-Aminoquinazolines substituted by a carbamic acid ester group present an interesting antiproliferative activity without tyrosine kinase inhibition. Thus, we drew the present study to explore the potential interaction of these molecules with the double-stranded DNA, the target of many conventional antitumor agents. We evaluated the strength and the way these molecules bind to DNA by UV-visible spectroscopy, circular dichroism, DNA thermal denaturation, and fluorescence measurements.

Keywords: 2-aminoquinazolines; Cancer; Intercalating agents; PD153035; Kinase inhibition

Abbreviations: ATP: Adenosine 5'-triphosphate; BET: Ethidium Bromide; CD: Circular Dichroism; DMSO: Dimethyl Sulfoxide; DNA: Deoxyribonucleic Acid; EGFR: Epidermal Growth Factor Receptor; Etoac: Ethyl Acetate; Etoh: Ethanol; FC: Flash Chromatography; Meoh: Methanol; Rt: Room Temperature; VEGFR: Vascular Endothelial Growth Factor Receptor

Introduction

Cancer is one of the most leading causes of mortality in the world, responsible of almost 13% of deaths worldwide. 12.7 million of new cancers were diagnosed in 2008, 7 million of them in developing countries [1]. There are different cancer treatments whose use depends on the nature and stage of the tumor. Chemotherapy is largely used since cancer cells grow and multiply much faster than most cells in the body. Many different chemotherapy drugs are available. Anti-neoplastic drugs are divided into five classes including alkylating agents, anti-metabolites, antitumor antibiotics, topoisomerase inhibitors and tubulin-binding drugs [2]. Unfortunately, these drugs discriminate between cancer cells and normal cells causing several side effects. Targeted therapies focus particular features of cancer cells, almost absent in normal cells. Although they target different receptors, they all interfere in the growth division, repair and/or communication of cancer cells with their environment. Modern targeted therapies include the use of monoclonal antibodies and kinase inhibitors [3,4]. They mainly target transmembrane receptors like Epidermal Growth Factor Receptor (EGFR), member of the ErbB family and Vascular Endothelial Growth Factor Receptor-2 (VEGFR-2). Numerous studies demonstrated that aberrant expression or mutation of EGFR can lead to several cancers [5]. The VEGF receptors (especially VEGFR-2) are considered as important targets in antiangiogenic therapies in cancer treatments [6].

Quinazoline derivatives represent an attractive scaffold to design anticancer drugs because of their multiple biological activities, notably as kinase inhibitors [7]. The first generation of 4-anilinoquinazolines such as the compound PD153035 showed a high EGFR affinity but a low *in vivo* activity [8]. Many studies were performed in our team

around this 4-anilinoquinazoline scaffold and led to the determination of EGFR and/or VEGFR-2 tyrosine kinase inhibitors. The enzymatic and cellular results of the most active compounds are presented in Table 1 [9,10].

The halogenated derivatives (PD153035, **1** and **2**) showed an important EGFR inhibition. Among these compounds, only compound **2** inhibited the cancer cell growth, with IC₅₀ of 6.6, 6.7 and 4.9 μM on PC3, HT29 and MCF7, respectively. Substitution of the anilino group by a carbamic acid ester moiety leads to an interesting dual inhibition of EGFR and VEGFR-2. However, compounds **3**, **4** and **5** showed weak antiproliferative activities on the three used cancer cell lines (IC₅₀ > 10 μM).

In addition to these results and to the potential applications of the quinazoline core in anticancer drugs, complementary studies were carried out. We studied the impact of an amino group in C-2 position of the quinazoline core for increasing the solubility of compounds in order to improve affinity for EGFR and/or VEGFR-2. For this reason, a series of 2-amino-4-anilinoquinazolines was designed, synthesized and biologically assessed (Figure 1).

Chemistry

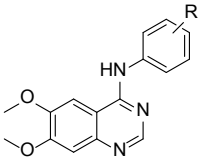
The synthesis of the 4-chloro-2-aminoquinazoline (**7**) is illustrated in Figure 2. Reaction of commercial methyl 4,5-dimethoxyanthranilate with cyanamide using concentrated HCl as catalyst gave the compound **6** [11]. The quinazolinone (**6**) was converted to 4-chloro-2-amino-

***Corresponding author:** Laurence Goossens, Institut de Chimie Pharmaceutique Albert Lespagnol, EA GRITA, 3 rue du Professeur Laguesse, B.P. 83, 59006 Lille, France, Tel: +33-3-20-96-47-02; Fax: +33-3-20-96-49-06; E-mail: laurence.goossens@univ-lille2.fr

Received January 19, 2015; Accepted February 16, 2015; Published February 18, 2015

Citation: Ravez S, Schifano-Faux N, Barczyk A, Arsenlis S, Castillo Aguilera O, et al. (2015) Synthesis and Antiproliferative Activity of 2-amino-4-Anilinoquinazoline Derivatives. Med chem 5: 067-076. doi:10.4172/2161-0444.1000245

Copyright: © 2015 Ravez S, et al. This is an open-access article distributed under the terms of the Creative Commons Attribution License, which permits unrestricted use, distribution, and reproduction in any medium, provided the original author and source are credited.

	R	Enzymatic inhibition (IC ₅₀ , μM)		Cell growth inhibition (IC ₅₀ , μM)		
		EGFR ^b	VEGFR-2 ^c	PC3 ^a	HT29 ^a	MCF7 ^a
						
PD153035	3-Br	0.0005	0.42	>10	>10	>10
1	3-Br,4-CH ₃	0.56	>10	>10	>10	>10
2	3-Cl,4-F	0.40	5.30	6.6 ± 1.70	6.7 ± 0.78	4.9 ± 0.54
3	4-NHCOOCH ₃	6.90	5.80	>10	>10	>10
4	3-CH ₃ ,4-NHCOOC ₂ H ₅	0.90	0.65	>10	>10	>10
5	3-Cl,4-NHCOOC ₂ H ₅	1.00	0.50	9.8 ± 0.35	>10	>10

^a The cell growth rate was evaluated by performing the MTS assay. Data are represented as the mean ± SEM of at three experiments performed in triplicate. Higher concentrations were not used to avoid precipitation of the compound in the culture medium

^bInhibition of EGFR (purified from human carcinoma A431 cells) tyrosine kinase activity

^cInhibition of VEGFR-2 (recombinant protein) tyrosine kinase activity

Table 1: Enzymatic and cell growth inhibition results of quinazoline derivatives.

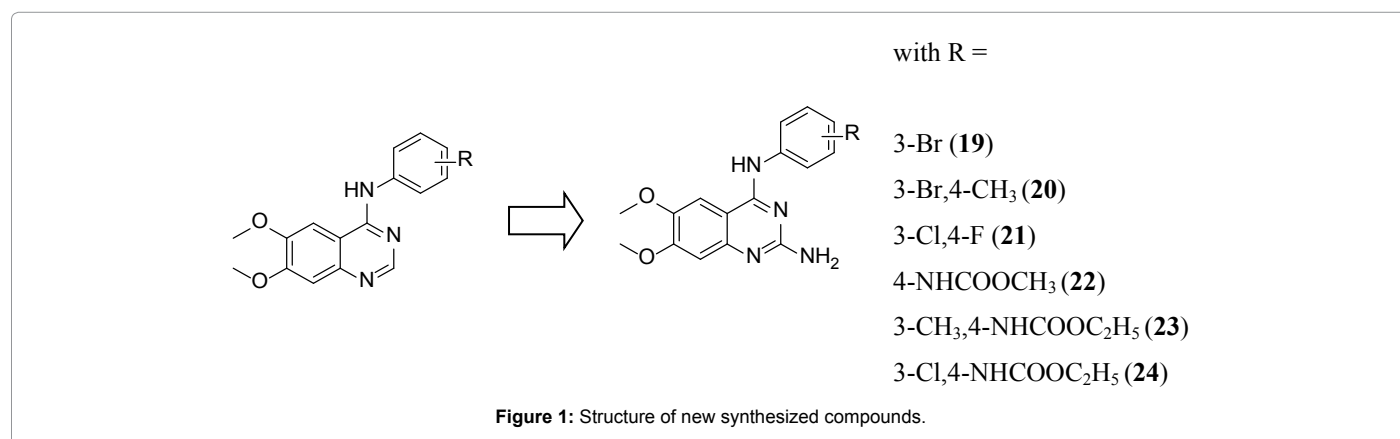
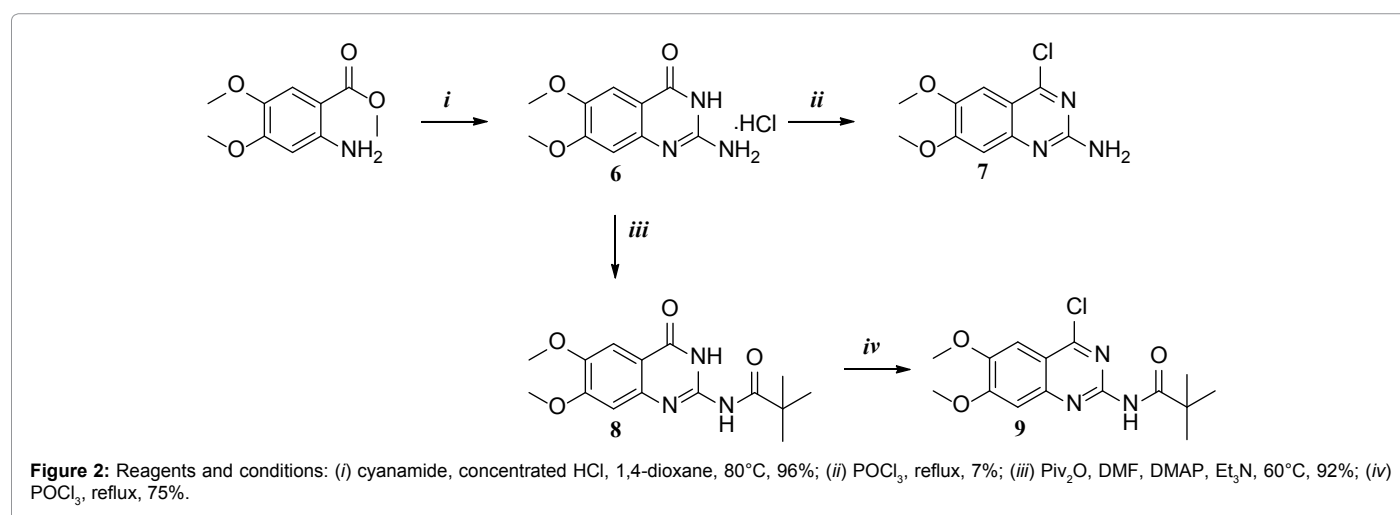
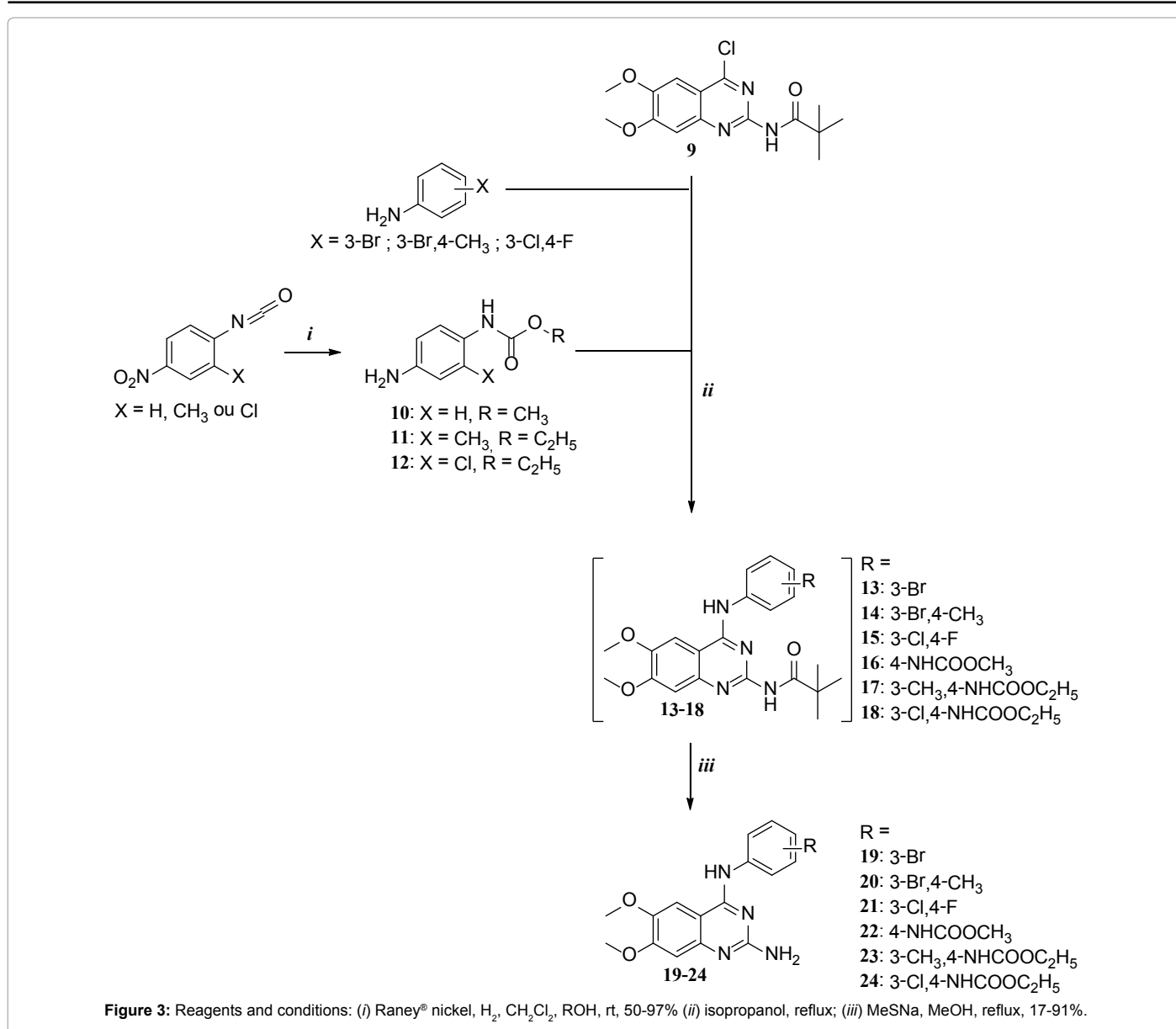


Figure 1: Structure of new synthesized compounds.



quinazoline (7) with POCl₃ in 7% yield [12]. The low yield of this step was probably due to the reaction between 2-amino group and POCl₃. Protection of the 2-amino moiety was therefore considered using the pivalic anhydride in the presence of DMAP and Et₃N to give compound 8 with good yield [13]. Chlorination with POCl₃ of protected quinazolinone (8) led to the key intermediate 4-chloroquinazolinone (9) in 75% yield.

As depicted in Figure 3, the synthesis of (aminophenyl)-carbamic acid esters 10-12 was performed by a one-pot reduction procedure of the corresponding nitrophenylisocyanate in the presence of various alcohols in CH₂Cl₂. This approach has been reported to be efficient and provided good yields and short reaction times [14]. Displacement of the chloro substituent of compound 8 with commercial or previously synthesized anilines in refluxing isopropanol led to the corresponding



4-anilinoquinazolines [15-17]. Deprotection of the 2-pivaloyl group was performed with sodium thiomethoxide in methanol to provide the target compounds (19-24).

The *N*-(Methyl-anilino)-6,7-dimethoxyquinazoline 25 was synthesized in two steps (Figure 4). First, the methylation of protected compound 18 in the presence of iodomethane and sodium hydride in *N,N*-dimethylformamide allowed to obtain *N*-(methyl-anilino)quinazoline intermediary. Deprotection of the 2-pivaloyl group was performed with sodium thiomethoxide in methanol to provide the target compound 25.

Experimental Section

Biological assays and methods

In vitro kinase assays: Kinase assays were performed in 96-well plates (Multiscreen Durapore. Millipore) using [γ -³²P]ATP (Perkin Elmer) and the synthetic polymer poly(Glu4/Tyr) (Sigma Chemicals) as a phosphoracceptor substrate. Tested compounds were dissolved in

DMSO. The final concentration of DMSO in assay solutions was 0.1%, which was shown to have no effect on kinase activity.

a) EGFR tyrosine kinase activity: 20 ng of EGFR (purified from human carcinoma A431 cells, Sigma Chemicals) were incubated for 1 h at 28 °C using various concentrations of tested compounds in kinase buffer (HEPES 50 mM pH 7.5, BSA 0.1 mg/mL, MnCl₂ 10 mM, MgCl₂ 5 mM, Na₃VO₄ 100 μM, DTT 0.5 mM, poly(Glu4/Tyr) 250 μg/mL, ATP 5 μM, [γ -³²P]ATP 0.5 μCi).

b) VEGFR-2 tyrosine kinase activity: 10 ng of VEGFR-2 (Recombinant Human Protein, Invitrogen) were incubated for 1 h at 28°C using various concentrations of tested compounds in kinase buffer (Tris 50 mM pH 7.5, BSA 25 μg/mL, MnCl₂ 1.5 mM, MgCl₂ 10 mM, DTT 2.5 mM, Na₃VO₄ 100 μM, β-glycerophosphate 5 mM, poly(Glu4/Tyr) 250 μg/mL, ATP 5 μM, [γ -³²P]ATP 0.5 μCi).

The reaction was stopped by adding 20 μL of trichloroacetic acid, 100%. Wells were washed 10 times with trichloroacetic acid, 10%. Plates were counted in a Top Count (Perkin Elmer) for 1 min per well.

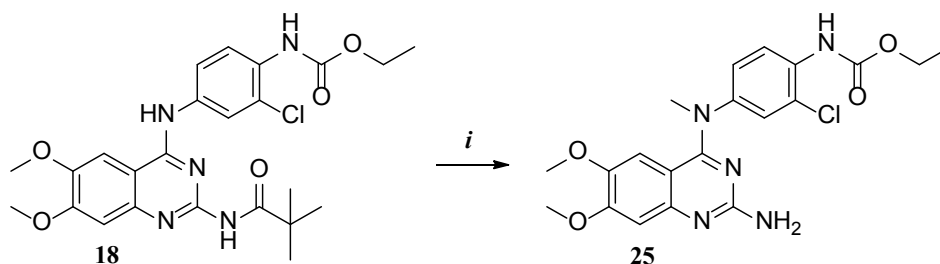


Figure 4: Reagents and conditions: (i) 1. CH_3I , NaH, DMF, rt 2. MeSNa, MeOH, reflux, 47%.

Cells and materials: Human PC3 prostate cancer cells, MCF7 breast cancer cells and HT29 colon cancer cells were obtained from European Collection of Cell Cultures. They were cultured, at 37°C in a CO_2 incubator, respectively in RPMI-1640, MEM and DMEM + Glutamax-I medium supplemented with 10% fetal bovine serum, penicillin (100 IU/mL) and streptomycin (100 $\mu\text{g}/\text{mL}$). FBS, medium, penicillin-streptomycin, and other agents used in cell culture studies were purchased from Invitrogen.

Cell proliferation: Briefly, cells were plated at a density of 3×10^3 cells/well in 96-well plates for 24h. Then the medium was removed, and cells were treated with either DMSO as a control or various concentrations of compounds. The final concentration of DMSO in the medium was <0.1% (v/v). After the cells were incubated for 72h, cell growth was estimated by colorimetric MTS test.

EGF stimulation: Briefly, HT29 cells were plated at a density of 3×10^3 cells/well in 96-well plates for 24h in DMEM medium supplemented with BSA 1%. Then, cells were treated with either DMSO as a control or compounds (1 μM). The final concentration of DMSO in the medium was <0.1% (v/v). After one hour, cells are stimulated with EGF (30 ng/mL), FBS (10%) or left untreated (BSA 1%). Then, the cells were incubated for 72h and cell growth was estimated by colorimetric MTS test.

Absorption spectroscopy and melting experiments studies: Absorption spectra and melting curves were obtained using an Uvikon 943 spectrophotometer coupled to a Neslab RTE111 cryostat. To perform the melting temperature (T_m) measurements, ctDNA was incubated alone (control T_m), then, each compound was incubated with ctDNA at a drug/ctDNA ratio of 1. Typically, 20 μM of the various drugs were prepared in 1 mL of BPE buffer (6 mM Na_2PO_4 , 2 mM NaH_2PO_4 , 1 mM EDTA, pH 7.1) in the presence of 20 μM of ctDNA and transferred into a quartz cuvette of 10 mm path length. The absorbance at 260 nm was measured every minute over the range 20-100°C with an increment of 1°C per minute and the spectra were recorded from 230 to 500 nm and referenced against a cuvette containing the same DNA concentration in the same buffer. The “melting” temperature T_m , deduced from melting curve, was taken as the midpoint of the hyperchromic transition and corresponds to the temperature for which half of the ctDNA is in single strand form and the other stays in the double strand form. DNA titrations were performed in the same buffer. To 1 mL of drug solution at 20 μM were added aliquots of a concentrated ctDNA solution (0-250 μM).

Circular dichroism: CD spectra were recorded on a Jasco J-810 spectrometer. Solutions of drugs, nucleic acids, and their complexes (1 mL in a 1 mM sodium cacodylate buffer, pH 7.0) were scanned in 10 mm quartz cuvettes. Measurements were made by progressive dilution of drug-DNA complex at a high P/D (phosphate/drug) ratio with a pure ligand solution to yield the desired drug/DNA ratio. Four scans

were accumulated and automatically averaged. Then 1 mL of drug solution at 50 μM was successively diluted with increased volumes of DNA at 200 μM .

Fluorescence titration experiments: Fluorescence titration data were recorded at room temperature using SPEX Fluorolog fluorometer. As 2-aminoquinazoline derivatives show weak fluorescence intensity variation with DNA titration, the binding studies were carried out through a competitive displacement fluorometry assay using DNA-bound ethidium bromide [18,19]. Excitation was set at 546 nm, and the fluorescence emission was monitored over the range 520-650 nm. Experiments were performed with an ethidium bromide/DNA molar ratio of 1.26:1 and a drug concentration range of 0.1-32 μM in a BPE buffer, pH 7.1. IC_{50} values for ethidium bromide displacement were calculated using a fitting function incorporated into GraphPad Prism 3.0 software, and the apparent binding constant was calculated as follows: $K_{\text{app}} = (1.26/\text{IC}_{50})K_{\text{ethidium}}$, with $K_{\text{ethidium}} = 10^7 \text{ M}^{-1}$.

General chemistry

Melting points were determined with a Büchi 535 capillary melting point apparatus and are uncorrected. Macherey Nagel Polygram® sil /G/UV₂₅₄ commercial plates were used for analytical TLC as well as UV light and/or with iodine to follow the course of the reaction. Flash chromatography (FC) was performed with silica gel Macherey Nagel Si 60, 0.015–0.040 mm. The structure of each compound was confirmed by IR (Bruker, FT-IR spectrometer ALPHA) and ^1H NMR (300 MHz, Bruker AC300P spectrometer). Chemical shifts (δ) are reported in parts per million downfield from TMS. J values are in hertz, and the splitting patterns are abbreviated as follows: s, singlet; d, doublet; t, triplet; q, quartet; m, multiplet. The purity of the compounds was tested by HPLC followed by APCI⁺ (atmospheric pressure chemical ionization) mass spectral detection on an LC-MS system, ThermoElectron Surveyor MSQ, and was >97%. HRMS experiments were performed on Q ExactiveBenchtop LC-MS (Thermo Scientific).

2-amino-6,7-dimethoxyquinazolin-4-one hydrochloride (6): Concentrated HCl (0.05 mL) was added dropwise to a solution of methyl 2-amino-4,5-dimethoxybenzoate (1 g, 4.73 mmol) and cyanamide (0.32 g, 7.57 mmol) in dioxane (40 mL) at room temperature. The mixture was heated at 80°C for 24 h and then cooled to room temperature. The precipitated was collected by filtration as a white solid (96%); mp>250°C. $\nu_{\text{max}}/\text{cm}^{-1}$ 3193 (NH_3^+), 1634 (C=O). ^1H NMR (DMSO-*d*₆) δ ppm 3.80 (s, 3H, OCH_3), 3.85 (s, 3H, OCH_3), 6.82 (s, 1H, ArH), 7.21 (brs, 2H, NH_2), 7.28 (s, 1H, ArH), 12.00 (brs, 1H, NH^+). LC-MS (APCI⁺), calcd for $\text{C}_{10}\text{H}_{11}\text{N}_3\text{O}_3$, m/z : 222 [(M + H)⁺].

2-amino-4-chloro-6,7-dimethoxyquinazolin-4-one (7): A solution of 2-amino-6,7-dimethoxyquinazolin-4-one hydrochloride (6) (1 g, 3.88 mmol) in phosphorus oxychloride (20 mL) was refluxed for 6 h. After removal of the solvent, the residue was dissolved in ice-water (50 mL) and the mixture was neutralized by 10% K_2CO_3 solution. The

precipitate was collected by filtration and dissolved in CH_2Cl_2 (100 mL). The organic layer was washed with 10% K_2CO_3 solution, brine and dried over CaCl_2 , and the solvent was removed under reduced pressure to give (7) as a white solid (7%); mp 194-196°C. $\nu_{\text{max}}/\text{cm}^{-1}$ 3105 (NH_2). $^1\text{H NMR}$ (CDCl_3) δ ppm 4.00 (s, 3H, OCH_3), 4.05 (s, 3H, OCH_3), 5.10 (brs, 2H, NH_2), 6.95 (s, 1H, ArH), 7.25 (s, 1H, ArH). LC-MS (APCI⁺), calcd for $\text{C}_{10}\text{H}_{10}\text{ClN}_3\text{O}_2$, m/z : 240 [(M + H)⁺ for ^{35}Cl] and 242 [(M + H)⁺ for ^{37}Cl].

2-pivaloylamino-6,7-dimethoxyquinazolin-4-one (8): To a solution of 2-amino-6,7-dimethoxyquinazolin-4-one hydrochloride (6) (2 g, 9.04 mmol) in DMF (40 mL) were added pivalic anhydride (5.05 g, 27.1 mmol), DMAP (0.05 g, 0.45 mmol), Et_3N (4.57 g, 45.2 mmol). The mixture was stirred at 60°C for 2 h and the solvent was removed under reduced pressure. The residue was dissolved in water and the mixture was neutralized by 10% K_2CO_3 . The precipitate was collected by filtration and dried in vacuo to give (8) as a white solid (92%); mp 159-161°C. $\nu_{\text{max}}/\text{cm}^{-1}$ 3050 (NH), 1672 (C=O). $^1\text{H NMR}$ (DMSO-*d*6) δ ppm 1.30 (s, 9H, *t*-Bu), 3.80 (s, 3H, OCH_3), 3.82 (s, 3H, OCH_3), 6.90 (s, 1H, ArH), 7.40 (s, 1H, ArH), 11.00 (brs, 1H, NH), 12.00 (brs, 1H, NH). LC-MS (APCI⁺), calcd for $\text{C}_{15}\text{H}_{19}\text{N}_3\text{O}_4$, m/z : 306 [(M + H)⁺].

2-pivaloylamino-4-chloro-6,7-dimethoxyquinazoline (9): A solution of 2-pivaloylamino-6,7-dimethoxyquinazolin-4-one (8) (2.55 g, 8.35 mmol) in phosphorus oxychloride (20 mL) was refluxed for 6 h. After removal of the solvent, the residue was dissolved in ice-water (50 mL) and the mixture was neutralized by 10% K_2CO_3 solution. The precipitate was collected by filtration and dissolved in CH_2Cl_2 (100 mL). The organic layer was washed with 10% K_2CO_3 solution, brine and dried over CaCl_2 , and the solvent was removed under reduced pressure to give (9) as a white solid (75%); mp 139-141°C. $\nu_{\text{max}}/\text{cm}^{-1}$ 3042 (NH), 1675 (C=O). $^1\text{H NMR}$ (DMSO-*d*6) δ ppm 1.30 (s, 9H, *t*-Bu), 4.00 (s, 3H, OCH_3), 4.05 (s, 3H, OCH_3), 7.20 (s, 1H, ArH), 7.40 (s, 1H, ArH), 10.20 (brs, 1H, NH). LC-MS (APCI⁺), calcd for $\text{C}_{15}\text{H}_{18}\text{ClN}_3\text{O}_3$, m/z : 324 [(M + H)⁺ for ^{35}Cl] and 326 [(M + H)⁺ for ^{37}Cl].

General procedure for (aminophenyl)carbamic acid esters (10-12): To a solution of corresponding commercial *p*-nitrophenylisocyanate (1 g) in 50 mL of a mixture of alcohol (MeOH or EtOH) and dichloromethane (5:5), was added Raney[®] nickel. After 18 h at room temperature in hydrogen atmosphere, the mixture was filtered. The solvent was removed under reduced pressure and the residue was purified by FC ($\text{CH}_2\text{Cl}_2/\text{AcOEt}$, 9:1).

***N*-(4-aminophenyl)carbamic acid methyl ester (10).** Beige solid (50%); mp 81-83°C. $\nu_{\text{max}}/\text{cm}^{-1}$ 3385 (NH_2), 1711 (C=O), 1265 (NH). $^1\text{H NMR}$ (DMSO-*d*6) δ ppm 3.60 (s, 3H, CH_3), 4.70 (brs, 2H, NH_2), 6.50 (d, 2H, $J=8.2$ Hz, 2 ArH), 7.00 (d, 2H, $J=8.2$ Hz, 2 ArH), 9.00 (brs, 1H, NH). LC-MS (APCI⁺), calcd for $\text{C}_8\text{H}_{10}\text{N}_2\text{O}_2$, m/z : 167 [(M + H)⁺].

***N*-(3-methyl-4-aminophenyl)carbamic acid ethyl ester (11).** Brown solid (97%); mp 90-93°C. $\nu_{\text{max}}/\text{cm}^{-1}$ 3382 (NH_2), 1710 (C=O), 1265 (NH). $^1\text{H NMR}$ (DMSO-*d*6) δ ppm 1.22 (t, 3H, $J=7.3$ Hz, CH_3), 2.19 (s, 3H, CH_3), 4.11 (q, 2H, $J=7.3$ Hz, CH_2), 5.33 (brs, 2H, NH_2), 7.12 (m, 2H, 2 ArH), 7.45 (d, 1H, $J=9.0$ Hz, ArH), 8.97 (brs, 1H, NH). LC-MS (APCI⁺), calcd for $\text{C}_{10}\text{H}_{14}\text{N}_2\text{O}_2$, m/z : 195 [(M + H)⁺].

***N*-(3-chloro-4-aminophenyl)carbamic acid ethyl ester (12):** Beige solid (84%); mp 109-111°C. $\nu_{\text{max}}/\text{cm}^{-1}$ 3385 (NH_2), 1711 (C=O), 1264 (NH). $^1\text{H NMR}$ (DMSO-*d*6) δ ppm 1.28 (t, 3H, $J=7.3$ Hz, CH_3), 4.05 (q, 2H, $J=7.3$ Hz, CH_2), 5.30 (brs, 2H, NH_2), 6.46 (dd, 1H, $J=2.3$ and 8.7 Hz, ArH), 6.61 (d, 1H, $J=2.3$ Hz, ArH), 6.97 (d, 1H, $J=8.7$ Hz, ArH), 8.52 (brs, 1H, NH). LC-MS (APCI⁺), calcd for $\text{C}_9\text{H}_{11}\text{ClN}_2\text{O}_2$, m/z : 215 [(M + H)⁺ for ^{35}Cl] and 217 [(M + H)⁺ for ^{37}Cl].

General procedure for 2-amino-4-anilino-6,7-dimethoxyquinazoline derivatives (19-24): To a solution of 2-pivaloylamino-4-chloro-6,7-dimethoxyquinazoline (8) (1 eq) in isopropanol, was added corresponding anilino derivatives (1,2 eq). After 2 h at reflux, the mixture was filtered. The obtained residue was stirred in methanol with sodium thiomethoxide at reflux for 2 h. The solvent was removed under reduced pressure. The residue was dissolved in water and the precipitate was collected by filtration and recrystallized to give desired compound.

2-amino-4-(3-bromoanilino)-6,7-dimethoxyquinazoline (19): Crystallization from acetonitrile gave pure 19 as white solid (91%); mp > 250°C. $\nu_{\text{max}}/\text{cm}^{-1}$ 3190 (NH_2). $^1\text{H NMR}$ (DMSO-*d*6) δ ppm 3.82 (s, 3H, OCH_3), 3.88 (s, 3H, OCH_3), 6.05 (br s, 2H, NH_2), 6.71 (s, 1H, ArH), 7.35 (m, 2H, 2 ArH), 7.63 (s, 1H, ArH), 8.05 (m, 2H, 2 ArH), 9.12 (br s, 1H, NH). LC-MS (APCI⁺), calcd for $\text{C}_{16}\text{H}_{15}\text{BrN}_4\text{O}_2$, m/z : 375 [(M + H)⁺ for ^{79}Br] and 377 [(M + H)⁺ for ^{81}Br]. HRMS (ESI (M+H)⁺ m/z) calcd for $\text{C}_{16}\text{H}_{15}\text{BrN}_4\text{O}_2$ 375.0451 found 375.0446.

2-amino-4-(3-bromo-4-methylanilino)-6,7-dimethoxyquinazoline (20): Crystallization from ethanol gave pure 20 as white solid (25%); mp > 250°C; $\nu_{\text{max}}/\text{cm}^{-1}$ 3193 (NH_2). $^1\text{H NMR}$ (DMSO-*d*6) δ ppm 2.30 (s, 3H, CH_3), 3.80 (s, 3H, OCH_3), 3.90 (s, 3H, OCH_3), 6.01 (br s, 2H, NH_2), 6.75 (s, 1H, ArH), 7.35 (d, 1H, $J=6.1$ Hz, ArH), 7.66 (s, 1H, ArH), 8.01 (m, 2H, 2 ArH), 9.10 (br s, 1H, NH). LC-MS (APCI⁺), calcd for $\text{C}_{17}\text{H}_{17}\text{BrN}_4\text{O}_2$, m/z : 389 [(M + H)⁺ for ^{79}Br] and 391 [(M + H)⁺ for ^{81}Br]. HRMS (ESI (M+H)⁺ m/z) calcd for $\text{C}_{17}\text{H}_{17}\text{BrN}_4\text{O}_2$ 389.0608 found 389.0606.

2-amino-4-(3-chloro-4-fluoroanilino)-6,7-dimethoxyquinazoline (21). Crystallization from acetonitrile gave pure 21 as white solid (17%); mp > 250°C. $\nu_{\text{max}}/\text{cm}^{-1}$ 3202 (NH_2). $^1\text{H NMR}$ (DMSO-*d*6) δ ppm 3.82 (s, 3H, OCH_3), 3.83 (s, 3H, OCH_3), 6.08 (br s, 2H, NH_2), 6.75 (s, 1H, ArH), 7.38 (m, 1H, ArH), 7.62 (s, 1H, ArH), 7.91 (m, 1H, ArH), 8.12 (m, H, ArH), 9.18 (br s, 1H, NH). LC-MS (APCI⁺), calcd for $\text{C}_{16}\text{H}_{14}\text{ClFN}_4\text{O}_2$, m/z : 349 [(M + H)⁺ for ^{35}Cl] and 351 [(M + H)⁺ for ^{37}Cl]. HRMS (ESI (M+H)⁺ m/z) calcd for $\text{C}_{16}\text{H}_{14}\text{ClFN}_4\text{O}_2$ 349.0862 found 349.0859.

***N*-[4-(2-amino-6,7-dimethoxyquinazolin-4-ylamino)phenyl]carbamic acid methyl ester (22).** Crystallization from ethanol gave pure 22 as white solid (90%); mp 197-199°C. $\nu_{\text{max}}/\text{cm}^{-1}$ 3356 (NH_2), 3304 (NH), 1710 (C=O). $^1\text{H NMR}$ (DMSO-*d*6) δ ppm 3.45 (s, 3H, CH_3), 3.95 (s, 3H, OCH_3), 4.00 (s, 3H, OCH_3), 6.01 (br s, 2H, NH_2), 7.50 (d, 2H, $J=8.9$ Hz, 2 ArH), 7.55 (s, 1H, ArH), 7.65 (d, 2H, $J=8.9$ Hz, 2 ArH), 8.20 (s, 1H, ArH), 9.10 (br s, 1H, NH), 9.50 (br s, 1H, NH). LC-MS (APCI⁺), calcd for $\text{C}_{18}\text{H}_{19}\text{N}_5\text{O}_4$, m/z : 370 [(M + H)⁺]. HRMS (ESI (M+H)⁺ m/z) calcd for $\text{C}_{18}\text{H}_{19}\text{N}_5\text{O}_4$ 370.1510 found 370.1509.

***N*-[2-methyl-4-(2-amino-6,7-dimethoxyquinazolin-4-ylamino)phenyl]carbamic acid ethyl ester (23).** Crystallization from acetonitrile gave pure 23 as white solid (90%); mp > 250°C. $\nu_{\text{max}}/\text{cm}^{-1}$ 3384 (NH_2), 3305 (NH), 1713 (C=O). $^1\text{H NMR}$ (DMSO-*d*6) δ ppm 1.25 (t, 3H, $J=7.6$ Hz, CH_3), 2.20 (s, 3H, CH_3), 3.90 (s, 3H, OCH_3), 3.95 (s, 3H, OCH_3), 4.15 (q, 2H, $J=7.6$ Hz, CH_2), 6.02 (br s, 2H, NH_2), 7.00 (s, 1H, ArH), 7.45 (Dd, 1H, $J=3.2$ and 9.0 Hz, ArH), 7.50 (D, 1H, $J=9.0$ Hz, ArH), 8.10 (s, 1H, ArH), 8.90 (d, 1H, $J=3.2$ Hz, ArH), 10.60 (br s, 1H, NH), 12.75 (br s, 1H, NH). LC-MS (APCI⁺), calcd for $\text{C}_{20}\text{H}_{23}\text{N}_5\text{O}_4$, m/z : 398 [(M + H)⁺]. HRMS (ESI (M+H)⁺ m/z) calcd for $\text{C}_{20}\text{H}_{23}\text{N}_5\text{O}_4$ 398.1823 found 398.1821.

***N*-[2-chloro-4-(2-amino-6,7-dimethoxyquinazolin-4-ylamino)phenyl]carbamic acid ethyl ester (24).** Crystallization from acetonitrile gave pure 24 as white solid (65%); mp > 250°C. $\nu_{\text{max}}/\text{cm}^{-1}$ 3380 (NH_2), 3304 (NH), 1707 (C=O). $^1\text{H NMR}$ (DMSO-*d*6) δ ppm 1.20 (t, 3H, $J=7.6$ Hz, CH_3), 3.80 (s, 3H, OCH_3), 3.85 (s, 3H, OCH_3), 4.10 (q, 2H, $J=7.6$ Hz, CH_2 , ArH), 6.00 (br s, 2H, NH_2), 6.70 (s, 1H, ArH), 7.40

(D, 1H, $J=8.9$ Hz, ArH), 7.60 (s, 1H, ArH), 7.90 (Dd, 1H, $J=3.1$ and 8.5 Hz), 8.00 (d, 1H, $J=2.9$ Hz, ArH), 8.90 (br s, 1H, NH), 9.15 (br s, 1H, NH). LC-MS (APCI⁺), calcd for C₁₉H₂₀ClN₅O₄, m/z : 418 [(M + H)⁺ for ³⁵Cl] and 420 [(M + H)⁺ for ³⁷Cl]. HRMS (ESI (M+H)⁺ m/z) calcd for C₁₉H₂₀ClN₅O₄ 418.1277 found 418.1274.

N-[2-chloro-4-(2-amino-6,7-dimethoxyquinazolin-4-N-(methyl)ylamino)phenyl]carbamic acid ethyl ester (25): A mixture of compound 18 (1 eq) and sodium hydride (60% in oil) (2 eq) in *N,N*-dimethylformamide (10 mL) was stirred 5 h at room temperature in a nitrogen atmosphere. Iodomethane (2 eq) was added, and the mixture was stirred for 16 h. The reaction was quenched by water, and then the aqueous solution was extracted with EtOAc, washed with a solution of K₂CO₃ 10%, and dried over MgSO₄. The solvent was removed under reduced pressure. The obtained residue was stirred in methanol with sodium thiomethoxide at reflux for 2 h. The solvent was removed under reduced pressure. The residue was dissolved in water and the precipitate was collected by filtration and recrystallized in methanol to give 25 as a white solid (47%); mp >250°C. ν_{\max} /cm⁻¹ 3321 (NH₂), 3310 (NH), 1792 (C=O). ¹H NMR (DMSO-*d*₆) δ ppm 1.22 (t, 3H, $J=7.6$ Hz, CH₃), 3.80 (s, 3H, OCH₃), 3.84 (s, 3H, OCH₃), 4.12 (q, 2H, $J=7.6$ Hz, CH₂), 6.03 (br s, 2H, NH), 6.73 (s, 1H, ArH), 7.88 (m, 1H, ArH), 7.68 (s, 1H, ArH), 8.02 (m, 2H, 2 ArH), 9.33 (br s, 1H, NH). LC-MS (APCI⁺), calcd for C₂₀H₂₂ClN₅O₄, m/z : 432 [(M + H)⁺ for ³⁵Cl] and 434 [(M + H)⁺ for ³⁷Cl]. HRMS (ESI (M+H)⁺ m/z) calcd for C₂₀H₂₂ClN₅O₄ 432.1433 found 432.1433.

Results and Discussion

Enzymatic inhibition and *in vitro* antiproliferative activity

Inhibitory activity against EGFR and VEGFR-2 tyrosine kinases of synthesized compounds was determined by measuring the *in vitro* levels of phosphorylation of the tyrosine-specific peptides (poly(Glu-Tyr)substrate) using [γ -³²P]ATP. The compounds were also evaluated for their antiproliferative activities towards three cancer cell lines: the hormone-independent PC3 prostate cancer cells, the MCF7 breast

cancer cells and the HT29 colon cancer cells, by MTS assay during 72 hours. Antiproliferative activities of compounds were compared to vandetanib, a dual EGFR/VEGFR-2 inhibitor. The data are summarized in Table 2.

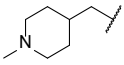
Incorporation of an amino group in C-2 position of 4-anilinoquinazolines substituted by one or two halogens increased antiproliferative activities of compounds despite a slight decrease of EGFR inhibition. Indeed, the halogenated compounds (19, 20 and 21) showed a good affinity for EGF receptor and an interesting inhibition of proliferation for the three studied cancer cell lines. A complementary study was performed to show the correlation between antiproliferative activity of the halogenated compound 21 (EGFR IC₅₀=0.13 μ M) and the EGFR inhibition. Indeed, the proliferation of HT29 cells was studied on several batches of cells: (a) control cells, (b) cells stimulated by Fetal Bovine Serum (FBS) containing many growth factors including EGF and (c) cells stimulated by growth factor EGF (Figure 5).

As shown in Figure 5, the EGF inhibitor PD153035, used as reference compound, and the compound 21 inhibited only the EGF-mediated cellular proliferation. As observed in Figure 5a, cell proliferation was not reduced by these inhibitors without FBS or EGF stimulation. So, the inhibition of cellular proliferation by the halogenated compound 21 could be due to its potential EGFR inhibition.

The introduction of an amino group in C-2 position of the quinazoline core in compounds 22, 23 and 24 led to a decrease of EGFR and VEGFR-2 inhibition (IC₅₀>10 μ M) and an increase of cell growth inhibition of three cancer cell lines. The 2-amino-4-anilinoquinazoline 24, with an ethyl carbamate in *para* and a chlorine in *meta* position on aniline, showed the best antiproliferative activities on PC3 (6.0 μ M), HT29 (3.6 μ M) and MCF7 (2.0 μ M). So, we also explored several studies to explain the antiproliferative effect of compound 24. These experiments are described in the following section.

DNA binding properties

A previous study, performed in our team demonstrated that

	R ₁	R ₂	R ₃	Enzymatic inhibitory (IC ₅₀ , μ M)		Cell growth inhibitory (IC ₅₀ , μ M)		
				EGFR ^a	VEGR-2	PC3 ^a	HT29 ^a	MCF7 ^a
vandetanib	2-F,4-Br	H		0.80	0.07	7.3	1.8	9.6
PD153035	3-Br	H	CH ₃	0.0005	0.42	>10	>10	>10
19	3-Br	NH ₂	CH ₃	1.80	>10	>10	3.7 ± 0.78	6.0 ± 1.67
1	3-Br,4-CH ₃	H	CH ₃	0.56	>10	>10	>10	>10
20		NH ₂	CH ₃	2.64	>10	4.8 ± 1.20	3.1 ± 0.89	3.6 ± 0.62
2	3-Cl,4-F	H	CH ₃	0.40	5.30	6.6 ± 1.70	6.7 ± 0.78	4.9 ± 0.54
21		NH ₂	CH ₃	0.13	>10	>10	6.2 ± 0.28	4.6 ± 0.55
3	4-NHCOOCH ₃	H	CH ₃	6.90	5.80	>10	>10	>10
22		NH ₂	CH ₃	>10	>10	7.6 ± 0.57	7.1 ± 0.61	8.6 ± 0.95
4	3-CH ₃ ,4-NHCOOC ₂ H ₅	H	CH ₃	0.90	0.65	>10	>10	>10
23		NH ₂	CH ₃	>10	>10	>10	7.2 ± 0.71	7.0 ± 0.91
5	3-Cl,4-NHCOOC ₂ H ₅	H	CH ₃	1.00	0.50	9.8 ± 0.35	>10	>10
24		NH ₂	CH ₃	>10	>10	6.0 ± 1.25	3.6 ± 2.51	2.0 ± 0.30

^aThe cell growth rate was evaluated by performing the MTS assay. Data are represented as the mean \pm SEM of at three experiments performed in triplicate. Higher concentrations were not used to avoid precipitation of the compound in the culture medium

^bInhibition of EGFR (purified from human carcinoma A431 cells) tyrosine kinase activity

^cInhibition of VEGFR-2 (recombinant protein) tyrosine kinase activity

Table 2: Enzymatic and cell growth inhibition results of 2-aminoquinazoline derivatives.

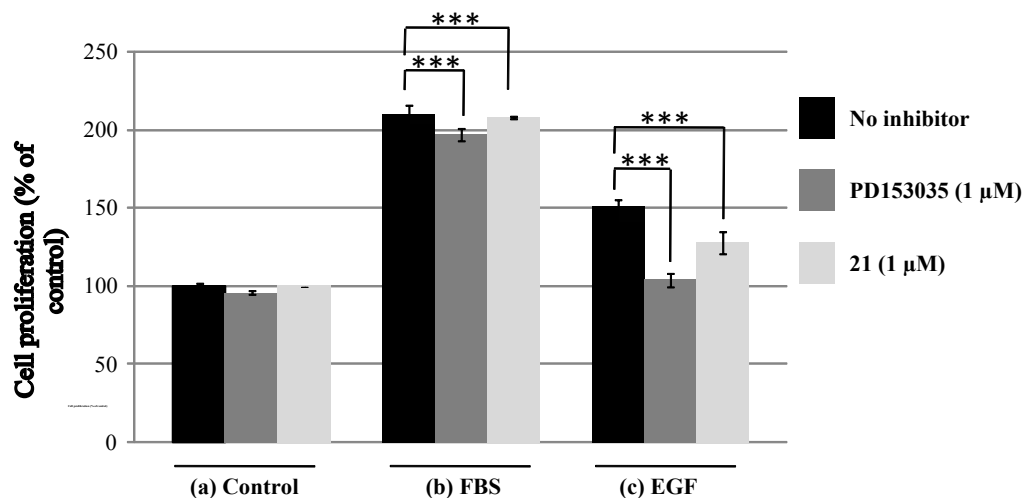


Figure 5: Percentage of HT29 cells untreated or treated by inhibitor (PD153035 and compound 21) under different conditions (FBS or EGF stimulation). The cell growth rate was evaluated by performing the MTS assay. Data are represented as the mean \pm SEM of at three experiments performed in triplicate (***) $p < 0.001$.

	R_1	R_2	R_3	ΔT_m ($^{\circ}\text{C}$)
5	H	H	3-Cl-4-NHCOOC ₂ H ₅	0
24	NH ₂	H	3-Cl-4-NHCOOC ₂ H ₅	8.1 \pm 0.8
25	NH ₂	CH ₃	3-Cl-4-NHCOOC ₂ H ₅	6.3 \pm 0.6
EBE-A22	H	CH ₃	3-Br	8.1 \pm 0.8

Variations in melting temperature ($\Delta T_m = T_m^{\text{Drug-DNA complex}} - T_m^{\text{DNA alone}}$) at drug/ctDNA ratio of 1.

Means values are calculated from at least two separate experiments with typical standard deviations of less than $\pm 10\%$.

Table 3: DNA thermal denaturation results.

4-(*N*-methyl)-anilinoquinazoline derivatives bound to ctDNA (calf thymus DNA) by an intercalative process [9,16]. Similarly we studied the capacity of the 2-aminoquinazoline 24 to bind to the DNA. To evaluate the role of the amino group in C-2 position in the interaction with ctDNA, we chose to test the 4-anilinoquinazoline 5 without amino group in C-2 position as reference. As shown previously [9], *N*-methylation increased interaction with ctDNA, so we also assessed the *N*-methyl analogue of 24 (compound 25), and an intercalator agent (EBE-A22), synthesized by us [16].

Therefore, we engaged different methods to study the binding mode to ctDNA for the newly synthesized compounds: DNA thermal denaturation, UV-visible spectroscopy, circular dichroism and fluorescence measurements.

DNA thermal denaturation experiments: The ability of the drugs to protect ctDNA against thermal denaturation was used as an indicator of their capacity to bind and to stabilize the DNA double helix. The ΔT_m values ($\Delta T_m = T_m^{\text{Drug-DNA complex}} - T_m^{\text{DNA alone}}$) are presented in Table 3.

The compound 24 show a ΔT_m value of 8.1 $^{\circ}\text{C}$ which indicates a stabilization of DNA against heat denaturation. This compound displays the same value that the reference intercalator compound EBE-A22. The comparison of results obtained for compounds 5 and 24 shows that incorporation of an amino group in C-2 position on 4-anilinoquinazolines is considered as a positive element to observe

DNA interaction, probably due to additional electrostatic interactions involving DNA phosphodiester groups. Contrary to previous results [10], the *N*-methylation in 4-position of the 2-amino-4-anilinoquinazoline did not improve the DNA interaction (25 vs. 24).

UV-Visible spectroscopy: The binding of four compounds was studied by UV-visible spectroscopy. Figure 6 displays UV absorption measurements recorded upon ctDNA titration into a buffered aqueous solution.

Addition of ctDNA induced few marked changes of the absorption spectrum of the compound 5 considered as a negative control. The spectrum of the 2-amino analogue (24) varied with DNA titration as illustrated by bathochromic and hypochromic shifts and an absorption maximum red-shifted from 350 to 370 nm. An isobestic point at 382 nm was detected pointing to the existence of a single binding mode. The UV-visible spectrum of compound 25 showed also bathochromic and hypochromic shifts but no clear isobestic point was spotted.

Circular dichroism (CD): Preliminary evaluations showed a potential interaction between the compounds 24 or 25 and ctDNA. To confirm these results and to define more precisely the binding process, a spectroscopic method utilizing polarized light and CD measurements was performed. The CD spectra of ctDNA or studied compounds are characterized by no change of ellipticity (Θ) between 320 and 420 nm (data not shown). The intensity changes of ellipticity are usually the

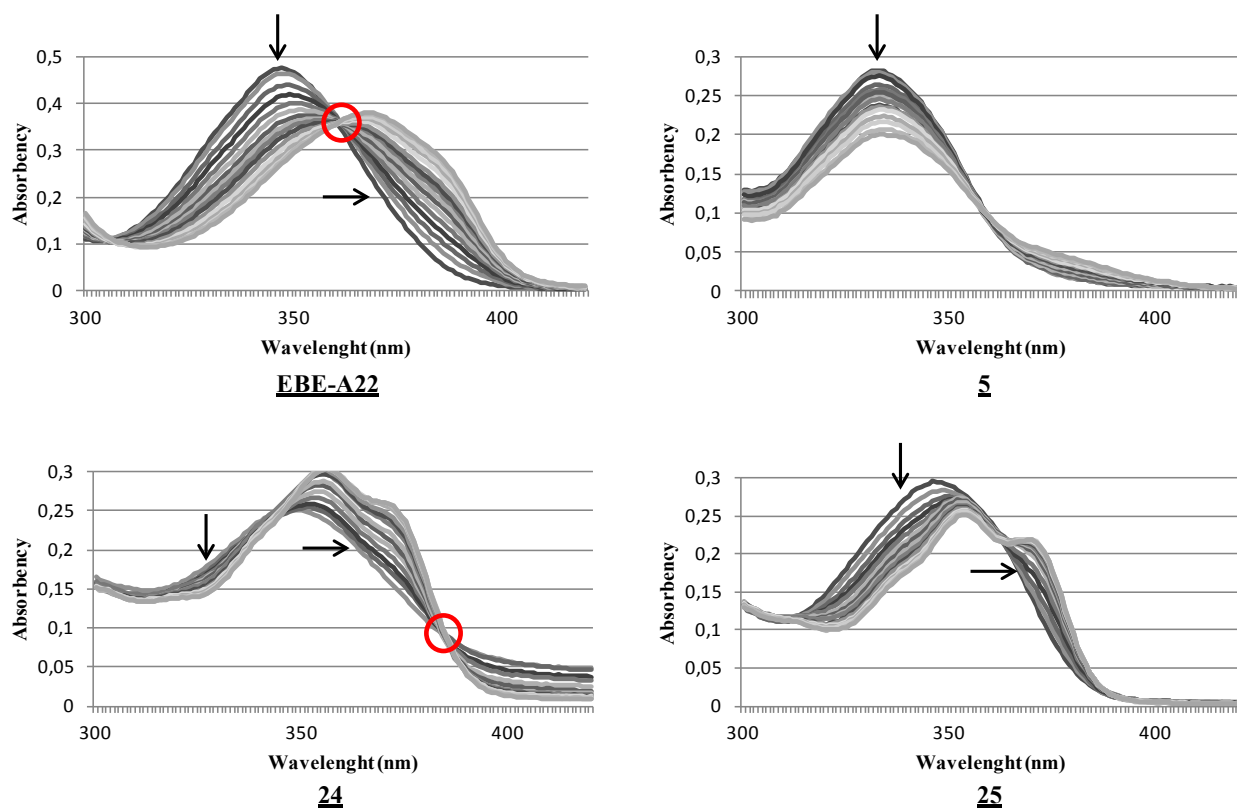


Figure 6: UV-visible spectra of drug at the concentration of 20 μM upon addition of ctDNA (0-250 μM) in BPE buffer (pH 7.1). Figure depicting the fitting plots obtained between 300 and 420 nm. Arrows correspond to hypochromic (\downarrow) and bathochromic (\rightarrow) effects, respectively. Red rings localize the isobestic point.

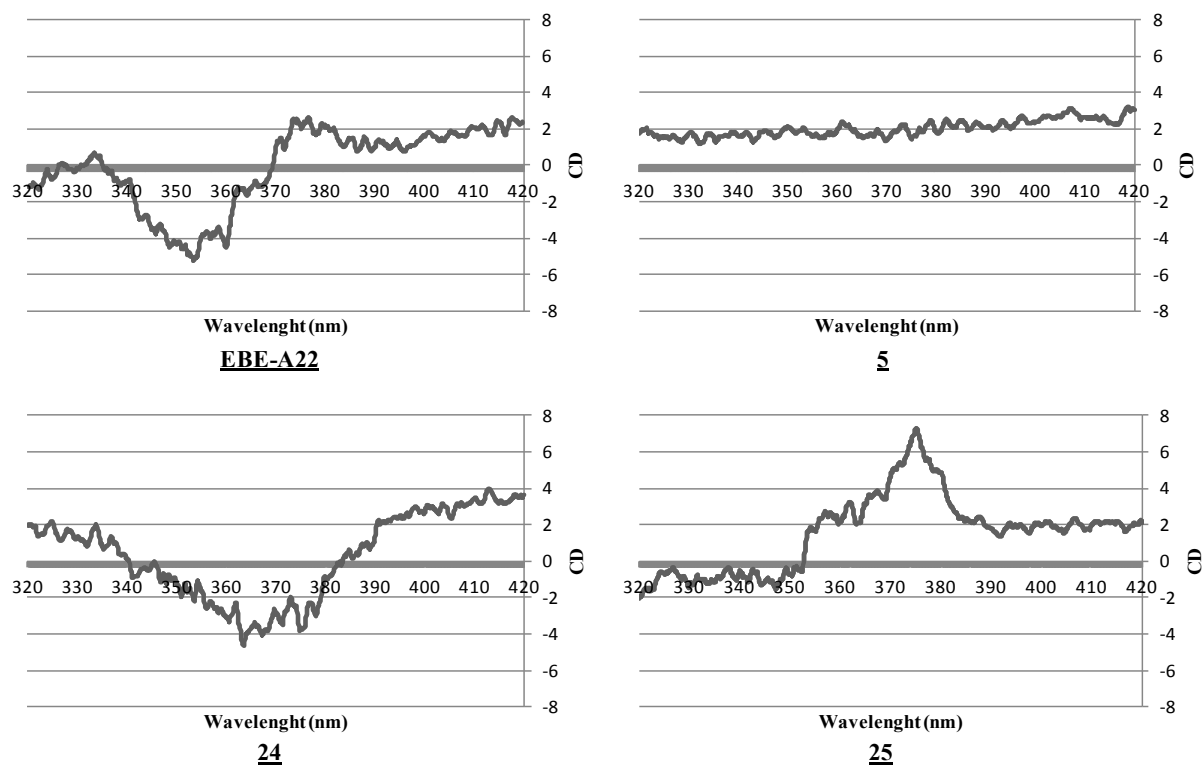


Figure 7: Circular dichroism spectra of ctDNA (200 μM) in the presence of drug (50 μM) in cacodylate buffer (1 mM, pH 7.04). Figure depicting the fitting plots obtained between 320 and 420 nm.

result of the interaction of drugs with ctDNA. Solutions of DNA in the presence of drugs were analyzed by CD (Figure 7).

As depicted in Figure 7, no variation of ellipticity was observed on the spectrum of the compound 5 in the presence of DNA, pointing no interaction between this compound and ctDNA. However, for compounds 24, 25 or EBE-A22, variations of ellipticity were observed in the spectral range 320-420 nm. CD measurements of EBE-A22 and 24 showed a similar negative band centered at 352 and 362 nm respectively. This typical negative CD is consistent with an intercalative DNA binding mode. The *N*-methylation of 24 induced a failover of CD signal. Indeed, a positive band centered at 375 nm was observed on the spectrum of 25. This intensity change could be the result of the interaction of 25 with the DNA minor groove [17].

Fluorescence measurements: DNA binding affinity of compound 24 was quantified by means of fluorescence K_{app} (Figure 8). As a weak fluorescence was observed upon DNA titration, an indirect method was privileged.^{18,19} We used the conventional fluorescence quenching assay based on DNA binding competition between the intercalating drug ethidium bromide (BET) and the tested molecule. Indeed, BET is an efficient DNA intercalator and its interaction with DNA causes highly fluorescence emission. The binding ability of drugs to form a drug-DNA complex can be determined from the displacement of BET, causing a quenching of the fluorescence signal due to the dissolved oxygen in aqueous solution.

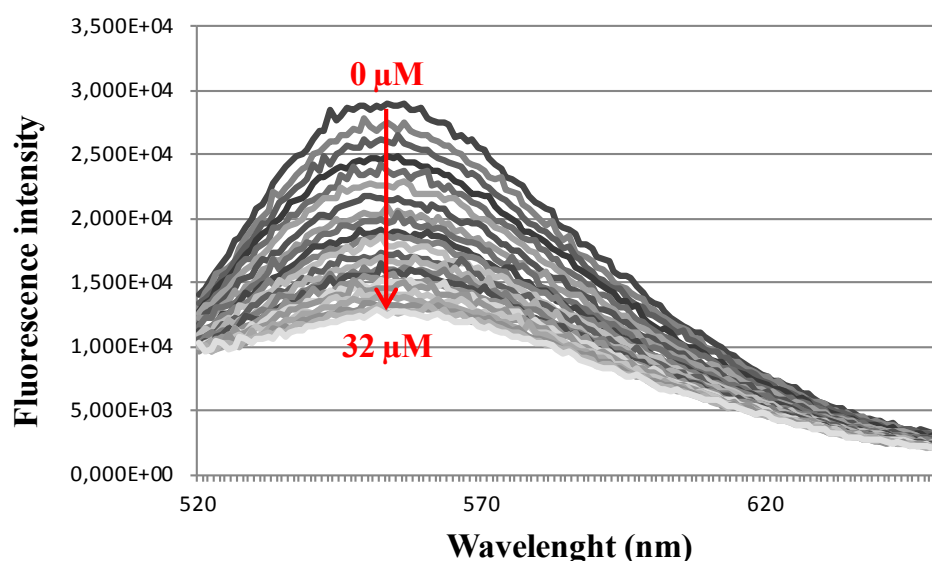
The fluorescence quenching shown in Figure 8 revealed that the

compound 24 was able to displace BET by competitive binding in the same DNA intercalation site. Fluorescence variations induced by addition of drug allowed the determination of the apparent binding constant (K_{app}) of 24 using nonlinear least-squares analysis (GraphPad Prism software): $K_{app[24]} = 1.39 \times 10^6 \pm 0.07 \times 10^6 \text{ M}^{-1}$. This data attests that 2-aminoquinazoline 24 is a potent DNA intercalating agent. For the compounds 5 and 25, fluorescence variation was too weak to calculate the apparent binding constant (Supplementary file).

We have studied the binding mode of several compounds by DNA thermal denaturation, UV-visible spectroscopy, circular dichroism and fluorescence measurements. The obtained results revealed that the compound 24 presented a good affinity for DNA and led to a duplex stabilization (Table of Content).

Conclusions

In conclusion, a series of 2-aminoquinazolines substituted by different anilino groups in C-4 position was designed and synthesized. Most of the synthesized compounds inhibited the proliferation of the three studied cancer cell lines (PC3, prostate cancer; MCF7, breast cancer and HT29, colon cancer). Several studies were conducted to explain the antiproliferative effect. 2-Aminoquinazolines substituted in C-4 position by halogeno-aniline (19, 20 and 21) showed an EGFR tyrosine kinase inhibition with IC_{50} values at micromolar range, in correlation with their antiproliferative activities. Substitution of anilino group by a bulky group like carbamate triggered a loss of tyrosine kinase inhibition. However, the antiproliferative activities of carbamate



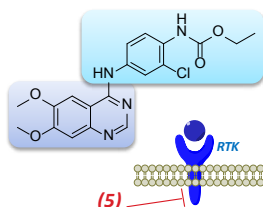
	K_{app}
5	0%*
24	$1.39 \times 10^6 \pm 0.07 \times 10^6 \text{ M}^{-1}$
25	12%*

*Fluorescence variations were too weak to calculate the apparent binding constant. Percentages represent the displacement of BET with 32 μM of compound 5 and 25.

Figure 8: Apparent binding constant measured by fluorescence using $[\text{BET}]/[\text{DNA}] = 1.26$. Fluorescence spectra of DNA-BET complex ($\lambda_{ex} = 546 \text{ nm}$) upon addition of drug (0.1-32 μM) in BPE buffer (pH 7.1). Figure depicting the fitting plots obtained between 520 and 650 nm.

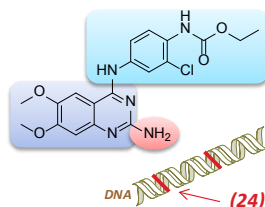
Table of Contents Entry

Dual EGFR/VEGFR-2 inhibitor No antiproliferative activities



+NH₂
in C-2
position

Intercalating agent Antiproliferative activities



Here, we report the highlighting of 2-aminoquinazoline scaffold as DNA intercalating agents for cancer therapy

derivatives could be explained by their interaction with DNA highlighted by several studies: DNA thermal denaturation, UV-visible spectroscopy, circular dichroism and fluorescence measurements. The various spectra revealed that compound 24 is a DNA intercalating agent. However, the affinity of the 2-amino-4-anilinoquinazoline 24 for DNA is lower compared to classical potent intercalators such as ethidium bromide. Nevertheless, the DNA-binding studies confirmed that the 2-amino-4-anilinoquinazoline core is a suitable skeleton, allowing an effective DNA intercalative process. Further development for this series should include a series of 4-anilino-benzo-(1,2,3)-triazines or 2-aminomethyl-4-anilinoquinazolines.

Acknowledgements

Kinase assays were performed on the Binding-Platform of ICPAL, University of Lille 2, supported by PRIM (Pôle de Recherche Interdisciplinaire pour le Médicament). We thank the LaRMN, Faculty of Pharmacy, University of Lille 2. The authors thank Céline Lengart and Nathalie Duhal from the CUMA (Centre Universitaire de Mesures et d'Analyses), University of Lille 2, for mass spectrometry analysis.

References

1. Lopez-Gomez M, Malmierca E, de Gorgolas M, Casado E (2013) Cancer in developing countries: the next most preventable pandemic. The global problem of cancer. *Crit Rev Oncol Hematol* 88: 117-122.
2. Caley A, Jones R (2012) The principles of cancer treatment by chemotherapy. *Surgery* 30: 186-190.
3. Gerber DE1 (2008) Targeted therapies: a new generation of cancer treatments. *Am Fam Physician* 77: 311-319.
4. Wu HC, Chang DK, Huang CT (2006) Targeted Therapy for Cancer. *J Cancer Mol* 2: 57-66.
5. Ribeiro FA, Noguti J, Oshima CT, Ribeiro DA (2014) Effective targeting of the epidermal growth factor receptor (EGFR) for treating oral cancer: a promising approach. *Anticancer Res* 34: 1547-1552.
6. Shahneh FZ, Baradaran B, Zamani F, Aghebati-Maleki L (2013) Tumor angiogenesis and anti-angiogenic therapies. *Hum Antibodies* 22: 15-19.
7. Selvam TP, Kumar PV (2011) Quinazoline marketed drugs - a review. *RIP* 1: 1-21.
8. Fry DW, Kraker AJ, McMichael A, Ambroso LA, Nelson JM, et al. (1994) A specific inhibitor of the epidermal growth factor receptor tyrosine kinase. *Science* 265: 1093-1095.
9. Garofalo A, Goossens L, Baldeyrou B, Lemoine A, Ravez S, et al. (2010) Design, synthesis, and DNA-binding of N-alkyl(anilino)quinazoline derivatives. *J Med Chem* 53: 8089-8103.
10. Garofalo A, Goossens L, Lemoine A, Ravez S, Six P, et al. (2011) [4-(6,7-Disubstituted quinazolin-4-ylamino)phenyl] carbamic acid esters: a novel series of dual EGFR/VEGFR-2 tyrosine kinase inhibitors. *Med Chem Commun* 2: 65-72.
11. Bridges AJ, Zhou H, Cody DR, Rewcastle GW, McMichael A, et al. (1996) Tyrosine kinase inhibitors. 8. An unusually steep structure-activity relationship for analogues of 4-(3-bromoanilino)-6,7-dimethoxyquinazoline (PD 153035), a potent inhibitor of the epidermal growth factor receptor. *J Med Chem* 39: 267-276.
12. Ruchelman AL, Houghton PJ, Zhou N, Liu A, Liu LF, et al. (2005) 5-(2-aminoethyl) dibenzo[c,h][1,6]naphthyridin-6-ones: variation of n-alkyl substituents modulates sensitivity to efflux transporters associated with multidrug resistance. *J Med Chem* 48: 792-804.
13. Gangjee A, Yang J, Ilnat MA, Kamat S (2003) Design, synthesis and biological evaluation of substituted pyrrolo[2,3-d]pyrimidines as multiple receptor tyrosine kinase inhibitors and antiangiogenic agents. *Bioorg Med Chem* 11: 5155-5170.
14. Garofalo A, Goossens L, Lebegue N, Depreux P (2011) Novel and Efficient One-Pot Synthesis of (Aminophenyl)carbamic Acid Esters. *Synthetic Commun* 41: 2007-2016.
15. Gazit A, Chen J, App H, McMahon G, Hirth P, et al. (1996) Tyrosine kinase inhibitors. 8. An unusually steep structure-activity relationship study of 4-anilidoquinazolines. *Bioorg Med Chem* 4: 1203-1207.
16. Goossens JF, Bouey-Bencteux E, Houssin R, Henichart JP, Colson P, et al. (2001) DNA interaction of the tyrosine protein kinase inhibitor PD153035 and its N-methyl analogue. *Biochemistry* 40: 4663-4671.
17. Aleksic MM, Kapetanovic V (2014) An overview of the optical and electrochemical methods for detection of DNA - drug interactions. *Acta Chim Slov* 61: 555-573.
18. Baguley BC, Denny WA, Atwell GJ, Cain BF (1981) Potential antitumor agents. 34. Quantitative relationships between DNA binding and molecular structure for 9-anilinoacridines substituted in the anilino ring. *J Med Chem* 24: 170-177.
19. Pavlov V, Kong Thoo Lin P, Rodilla V (2001) Cytotoxicity, DNA binding and localisation of novel bis-naphthalimidopropyl polyamine derivatives. *Chem Biol Interact* 137: 15-24.